

DR BIN TANG (Orcid ID : 0000-0002-3851-2330)

Article type : Rapid Communication

A New Low-Firing and High-Q Microwave Dielectric Ceramic $\text{Li}_9\text{Zr}_3\text{NbO}_{13}$

Han Yang^{1,2}, Bin Tang^{1,2,*}, Zixuan Fang^{1,2}, Jun Luo^{1,2}, Shuren Zhang^{1,2}

1. National Engineering Center of Electromagnetic Radiation Control Materials, University of Electronic Science and Technology of China.

2. State Key Laboratory of Electronic Thin Films and Integrated Devices, University of Electronic Science and Technology of China.

*corresponding author: tangbin@uestc.edu.cn

Abstract: The microwave dielectric ceramic $\text{Li}_9\text{Zr}_3\text{NbO}_{13}$ was found and investigated. Prepared via the solid-state reaction method, the $\text{Li}_9\text{Zr}_3\text{NbO}_{13}$ formed as a Li_2ZrO_3 -type solid solution at 880-900 °C, with monoclinic structure in C2/c space group and $Z = 4$. Typically, the $\text{Li}_9\text{Zr}_3\text{NbO}_{13}$ sintered at 900 °C exhibited the excellent microwave dielectric properties of $\epsilon_r = 21.3$, $Q \times f = 43,600$ GHz (at 7.4 GHz), $\tau_f = 7.3$ ppm/°C.

Key words: LTCC; microstructure; dielectric materials/properties

This article has been accepted for publication and undergone full peer review but has not been through the copyediting, typesetting, pagination and proofreading process, which may lead to differences between this version and the Version of Record. Please cite this article as doi: 10.1111/jace.15456

This article is protected by copyright. All rights reserved.

Introduction

Due to the importance of miniaturization and integration for microwave circuit system, the low-temperature co-fired ceramics (LTCC) technology has become an irreplaceable fabrication approach. Generally, high quality factor ($Q \times f > 10,000$ GHz), appropriate dielectric constant, near-zero temperature coefficient at the resonant frequency and low sintering temperature ($T < 961$ °C) should be indispensably taken into consideration to design the LTCC devices.¹⁻³ A series of Li-based dielectric ceramics, such as $\text{Li}_3\text{AlB}_2\text{O}_6$, Li_2WO_4 , Li_2ZrO_3 and Li_3NbO_4 ²⁻⁵ have been reported and utilized in practice. Among them, the Li_2ZrO_3 possesses $\varepsilon_r = 14.1$, $Q \times f = 17,640$ GHz and $\tau_f = +39.3$ ppm/°C, the Li_3NbO_4 sintered at 930 °C exhibits values of $\varepsilon_r = 15.8$, $Q \times f = 55,009$ GHz and $\tau_f = -49$ ppm/°C. There may exist some compounds with both good microwave dielectric properties and a low firing temperature between the Li_2ZrO_3 and Li_3NbO_4 in the $\text{Li}_2\text{O}-\text{ZrO}_2-\text{Nb}_2\text{O}_5$ system. With this purpose, the $(1-x)\text{Li}_3\text{NbO}_4-(x)\text{Li}_2\text{ZrO}_3$ ($0 \leq x \leq 1$) ceramic composites were investigated. At $x = 0.75$, the desirable ceramic $\text{Li}_{10}\text{Zr}_3\text{NbO}_{13}$ was found.

Experimental procedures

The ceramics were prepared by the solid-state reaction route. The stoichiometric mixtures of high purity ($>99.9\%$) Li_2CO_3 , ZrO_2 , Nb_2O_5 were milled with ethanol and zirconia balls for 4 h, the dried powders were calcined at 750 °C for 4 h. Later, the calcined powders were reground for 5 h, dried, mixed with polyvinyl alcohol, and then axially pressed into pellets with 15 mm in diameter and 7.5 mm in thickness under a pressure of 200 kg/cm² for 30 seconds. The pellets were sintered at different temperatures for 4 h with a heating rate of 5 °C /min.

The theoretical density (ρ_{theory}) was obtained from the Rietveld refinement and the bulk density (ρ_{bulk}) was measured by the Archimedes method. The relative density was calculated by:

$$\rho = \frac{\rho_{bulk}}{\rho_{theory}} \quad (1)$$

The phase composition was examined by X-ray diffraction (XRD) using CuK α radiation (Philips x'pert Pro MPD, Netherlands). The scanning electron microscopy (SEM) (FEI Inspect F, UK) was employed to study the micro-morphology. The microwave dielectric properties were measured by the Hakki–Coleman dielectric resonator method in TE011 mode using the network analyzer (Agilent Technologies E5071C, USA) and temperature chamber (DELTA 9023, Delta Design, USA). The τ_f was calculated by:

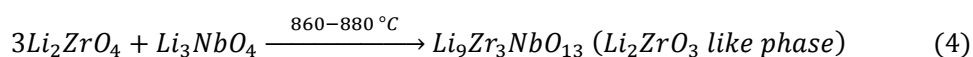
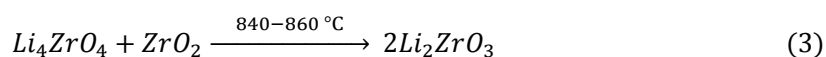
$$\tau_f = \frac{f_{t_2} - f_{t_1}}{f_{t_1} \times (t_1 - t_2)} \quad (2)$$

where f_{t_1} and f_{t_2} were the resonant frequencies at t_1 (25 °C) and t_2 (85 °C) respectively.

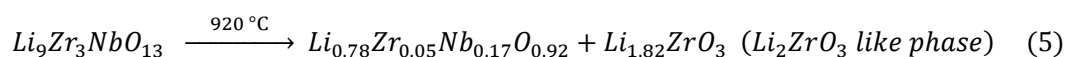
Results and discussion

Figure 1 shows the XRD patterns of the $(1-x)\text{Li}_3\text{NbO}_4-(x)\text{Li}_2\text{ZrO}_3$ ceramics sintered at 820-1150 °C for 4 h. The XRD results showed that while Li_2ZrO_3 forms an extensive range of solid solutions, Li_3NbO_4 forms little or no solid solutions. When $x \geq 0.45$, the Li_2ZrO_3 -type solid solutions were obtained, and a new low-firing and high-Q ceramic $\text{Li}_{1.9}\text{Zr}_3\text{NbO}_{13}$ lay at $x = 0.75$. The formula of the solid solution could be written as: $\text{Li}_{2+y}\text{Zr}_{1-4y}\text{Nb}_{3y}\text{O}_3$ ($0 < y \leq 0.16$), with the substitution mechanism of $4\text{Zr}^{4+} \rightleftharpoons \text{Li}^{1+} + 3\text{Nb}^{5+}$.⁶ When $x = 0.05\sim 0.35$, the two-phase composites of Li_3NbO_4 and Li_2ZrO_3 were obtained. Just when $x = 0$, the single-phase Li_3NbO_4 was formed.

Figure 2 shows the XRD patterns of the $\text{Li}_9\text{Zr}_3\text{NbO}_{13}$ ceramics sintered at 840-920 °C for 4 h, and Figure 3 described their phase constitutions. At 840 °C, the compounds consisted of Li_2ZrO_3 (#75-2157), Li_3NbO_4 (#82-1198), ZrO_2 (#87-2105) and Li_4ZrO_4 (#36-0121). The Li_2ZrO_3 presented as the main phase, with a content of 92.4%. At 860 °C, the Li_4ZrO_4 and ZrO_2 disappeared, the phase content of Li_3NbO_4 decreased, and the content of Li_2ZrO_3 increased to 94.9%. At 880 °C and 900 °C, only Li_2ZrO_3 phase was detected. This indicated that the $\text{Li}_9\text{Zr}_3\text{NbO}_{13}$ ceramics existed as a Li_2ZrO_3 -type solid solution at 880-900 °C:



At 920 °C, the $\text{Li}_{0.78}\text{Zr}_{0.05}\text{Nb}_{0.17}\text{O}_{0.92}$ (#42-0458) separated out, the pure Li_2ZrO_3 -type solid solution no longer maintained:



This revealed that the solubility of the $\text{Li}_9\text{Zr}_3\text{NbO}_{13}$ solid solution were sensitive to the sintering temperature.⁷

Figure 4 exhibits the crystal structures of prototypical Li_2ZrO_3 and Li_3NbO_4 . The refinements showed in Figure 5 were used to determinate the lattice parameters of the $\text{Li}_9\text{Zr}_3\text{NbO}_{13}$ ceramics. Similarly, the lattice parameters of the whole $\text{Li}_{2+y}\text{Zr}_{1-4y}\text{Nb}_{3y}\text{O}_3$ solid solution were obtained and listed in Table 1, and Figure 6 depicts their variation tendencies. The a, b, c and V_{unit} all gradually decreased with the increasing y. This should be attributed to the

obviously decreased sum of ionic radii in the substitution mechanism: $4\text{Zr}^{4+}(0.84\text{\AA}) \rightleftharpoons \text{Li}^{1+}(0.60\text{\AA}) + 3\text{Nb}^{5+}(0.74\text{\AA})$.

Figure 7 exhibits the SEM micrographs of the $\text{Li}_9\text{Zr}_3\text{NbO}_{13}$ ceramics sintered at 840-920 °C for 4 h. At 840 °C and 860 °C, the liquid phase was observed, the grains initially soaked in the liquid phase (Fig 7 (a)), then molded as irregular polygons (Fig 7 (b)). At 880 °C, the liquid phase disappeared, the grain boundaries became distinct, and the grains continuously grew up (Fig 7 (c)). The liquid phase should be Li_3NbO_4 and its phase transformation was just well consistent with both the SEM and XRD results. At 900 °C, a denser microstructure with grains in 3-5 μm was obtained (Fig 7 (d)). At 920 °C, the micrograph deteriorated with increased pores and shrank grains (Fig 7 (e)). The better images at 880 °C and 900 °C should be as a result of the forming of the Li_2ZrO_3 -type solid solution. The deteriorative image at 920 °C should be due to the phase transformation, the $\text{Li}_{0.78}\text{Zr}_{0.05}\text{Nb}_{0.17}\text{O}_{0.92}$ appeared, the pure-phase composition no longer existed.

Figure 8 shows the variation tendencies of the relative density, ε_r , $Q \times f$ and τ_f of the $\text{Li}_9\text{Zr}_3\text{NbO}_{13}$ ceramics as a function of the sintering temperature. The relative density continuously improved, and reached a maximum value of 93.67% at 900 °C, then sharply decreased at 920 °C. The continuous improvement could be attributable to the disappearance of the precursors with low density (Li_3NbO_4 , #82-1198, 3.94 g/cm³ and Li_4ZrO_4 , #36-0121, 3.87 g/cm³). While the decreased density at 920 °C should due to the appearance of the low-density $\text{Li}_{0.78}\text{Zr}_{0.05}\text{Nb}_{0.17}\text{O}_{0.92}$ (#42-0458, 2.51 g/cm³) and also the increased porosity (Fig 7 (e)). As

known to us, the density and ε_r were influenced by many same reasons such as the phase composition, pores and grain boundaries.⁸ Hence, in a similar trend, the ε_r increased from 20.1 to 21.3 at 840-900 °C, later dropped to 20.3 at 920 °C. The $Q \times f$ constantly increased and reached a maximum value of 43,600 GHz at 900 °C, then decreased at 920 °C. The τ_f value constantly decreased, reached a minimum value of 7.3 at 900 °C, then unfavorably increased at 920 °C. Notably, in the $\text{Li}_9\text{Zr}_3\text{NbO}_{13}$ ceramics, the change trend of microwave dielectric properties showed strong accordance with that of the phase content of Li_2ZrO_3 (Fig 3).⁹

Conclusion

There assuredly exist compound of $\text{Li}_9\text{Zr}_3\text{NbO}_{13}$ with advantages of both good microwave dielectric properties and a low-firing temperature in the $\text{Li}_2\text{O}-\text{ZrO}_2-\text{Nb}_2\text{O}_5$ system. The $\text{Li}_9\text{Zr}_3\text{NbO}_{13}$ existed as a Li_2ZrO_3 -type solid solution at 880-900 °C. Typically, the $\text{Li}_9\text{Zr}_3\text{NbO}_{13}$ sintered at 900 °C exhibited the excellent properties of $\varepsilon_r = 21.3$, $Q \times f = 43,600$ GHz (at 7.4 GHz), $\tau_f = 7.3$ ppm/°C, which shows highly potential for practical applications.

Acknowledgments

This work was supported by National Natural Science Foundation of China (Grant No 51672038).

References

1. Zhou D, Pang L-X, Wang D, et al. High permittivity and low loss microwave dielectrics suitable for 5G resonators and low temperature co-fired ceramic architecture. *J Mater Chem C*. 2017;5:10094-10098.
2. Ohashi M, Ogawa H, Kan A, Tanaka E. Microwave dielectric properties of low-temperature sintered $\text{Li}_3\text{AlB}_2\text{O}_6$ ceramic. *J Eur Ceram Soc*. 2005;25:2877-2881.
3. Zhou D, Randall CA, Pang L-X, et al. Microwave dielectric properties of Li_2WO_4 ceramic with ultra-low sintering temperature. *J Am Ceram Soc*. 2011;94:348-350.
4. Pang L-X, Zhou D. Microwave dielectric properties of low-firing Li_2MO_3 (M=Ti, Zr, Sn)

ceramics with B₂O₃–CuO Addition. *J Am Ceram Soc.* 2010;93:3614-3617.

5. Zhou D, Wang H, Pang L-X, et al. Microwave dielectric characterization of a Li₃NbO₄ ceramic and its chemical compatibility with silver. *J Am Ceram Soc.* 2008;91:4115-4117.
6. Aragon-Pia A, Villafuerte-Castrejn M, Valenzuela R, et al. Solid solutions with rock salt related structures on the join Li₂TiO₃-Li₃NbO₄. *J Mater Sci Lett.* 1984;3:893-896.
7. Fang Z-X, Tang B, Si F, Zhang S-R. Temperature stable and high-Q microwave dielectric ceramics in the Li₂Mg₃-xCaxTiO₆ system (x=0.00–0.18). *Ceram Int.* 2017;43:1682-1687.
8. Yu S-Q, Tang B, Zhang S-R, et al. Improved high-Q microwave dielectric ceramics in CuO-doped BaTi₄O₉-BaZn₂Ti₄O₁₁ system. *J Am Ceram Soc.* 2012;95:1939-1943.
9. Chen H-T, Tang B, Zhang S-R, et al. A novel formula for the quality factor calculation for the multiphase microwave dielectric ceramic mixtures. *J Eur Ceram Soc.* 2017;37:3347-3352.

Captions:

Figure 1. The XRD patterns of the (1-x)Li₃NbO₄-(x)Li₂ZrO₃ ceramics sintered at 820-1150 °C for 4 h.

Figure 2. The XRD patterns of the Li₉Zr₃NbO₁₃ ceramics sintered at 840-920 °C for 4 h.

Figure 3. The phase constitutions of the Li₉Zr₃NbO₁₃ ceramics sintered at 840-920 °C for 4 h.

Figure 4. The crystal structures of Li₂ZrO₃ and Li₃NbO₄

Figure 5. The refinements of the Li₉Zr₃NbO₁₃ solid solution sintered at 880 °C and 900 °C for 4 h. Circles are collected data, solid lines are fitted. Differences between them are shown below. Vertical marks indicate calculated peak positions.

Figure 6. The variation tendencies of lattice parameters of the Li_{2+y}Zr_{1-4y}Nb_{3y}O₃ solid solution, as a function of the y value with (a) a and b, (b) c and V_{unit}.

Figure 7. The SEM images of the surfaces of the Li₉Zr₃NbO₁₃ ceramics sintered at 840-920 °C for 4 h with (a) 840 °C, (b) 860 °C, (c) 880 °C, (d) 900 °C, (e) 920 °C. The small illustrations are cross sections

Figure 8. The variation tendencies of relative density and microwave dielectric properties of the Li₉Zr₃NbO₁₃ ceramics, as a function of sintering temperature with (a) relative density and ϵ_r , (b) $Q \times f$ and τ_f .

Table 1. The Lattice Parameters of the Li_{2+y}Zr_{1-4y}Nb_{3y}O₃ solid solution.

Table 1. The Lattice Parameters of the $\text{Li}_{2+y}\text{Zr}_{1-4y}\text{Nb}_3\text{O}_3$ Solid Solution

y (mol)	Lattice parameters (Å)			β (°)	Vol (Å ³)
	a	b	c		
0	5.425	9.031	5.423	112.691	245.120
0.016	5.422	9.014	5.415	112.748	244.064
0.048	5.421	9.009	5.399	112.699	243.221
0.077	5.420	9.001	5.398	112.700	243.178
0.104	5.411	9.000	5.396	112.680	242.453
0.130	5.407	8.997	5.393	112.677	242.104
0.155	5.405	8.996	5.393	112.656	241.990

